J. Biochem. **134**, 739–749 (2003)
DOI: 10.1093/jb/mvg202

A Novel Metalloprotease from *Gloydius halys* Venom Induces Endothelial Cell Apoptosis through Its Protease and Disintegrin-Like Domains

Weon-Kyoo You[1], Hyun-Ji Seo[1], Kwang-Hoe Chung[2] and Doo-Sik Kim[*,1]

[1]Dept. of Biochemistry, College of Science, Yonsei University, Seoul 120-749, Korea; and [2]Cardiovascular Research Institute, Yonsei University, College of Medicine, Seoul 120-752, Korea

Received September 8, 2003; accepted September 12, 2003

A novel hemorrhagic metalloprotease, halysase, isolated from the snake venom of *Gloydius halys* induces apoptosis in endothelial cells. The purified metalloprotease is a monomeric glycoprotein with an isoelectric point of 4.8. Analysis of the cDNA sequence encoding halysase revealed that the enzyme consists of multifunctional domains including a proprotein domain, a protease domain, a disintegrin-like domain and a cysteine-rich domain. The metalloprotease has a DECD sequence in the disintegrin-like domain instead of the typical RGD sequence. Halysase strongly inhibits proliferation of human umbilical vein endothelial cells in a dose-dependent manner as well as adhesion of the cells to extracellular matrix proteins. The enzyme specifically hydrolyzes not only extracellular matrix proteins such as fibronectin, vitronectin, and type IV collagen, but also integrins α1β1 and α5β1. The apoptosis of endothelial cells induced by halysase is closely associated with activation of caspase-3 and decreased level of Bcl-X_L/Bax. Apohalysase, which lacks metalloprotease activity, is also able to induce the apoptosis. Several lines of experimental evidence suggest that the protease domain and the disintegrin-like domain of halysase cooperatively contribute to the induction of endothelial cell apoptosis.

Key words: apoptosis, disintegrin-like domain, endothelial cell, hemorrhagic metalloprotease, protease domain.

Abbreviations: ADAM, a disintegrin and metalloprotease; BSA, bovine serum albumin; bFGF, basic fibroblast growth factor; CIM, cysteine-isoleucine-methionine; CVM, cysteine-valine-methionine; DECD, aspartate-glutamate-cysteine-aspartate; ECM, extracellular matrix; EDTA, ethylenediaminetetraacetic acid; FBS, fetal bovine serum; HUVEC, human umbilical vein endothelial cell; MDC, metalloprotease/disintegrin/cysteine-rich; NC, nitrocellulose; NLT, asparagine-leucine-threonine; PARP, poly ADP-ribose polymerase; PAS, periodic acid-Schiff's reagent; PBS, phosphate-buffered saline; PMSF, phenylmethanesulfonyl fluoride; PVDF, polyvinylidine difluoride; SECD, serine-glutamate-cysteine-aspartate; SDS-PAGE, sodium dodecyl sulfate-polyacrylamide gel electrophoresis; TCA, trichloroacetic acid.

Integrin-mediated cell adhesion to extracellular matrix (ECM) plays an important role in regulating cell survival and proliferation of anchorage-dependent cells such as epithelial and endothelial cells (*1*). Cell-cell and cell-extracellular matrix interactions provide cells with essential information for controlling morphogenesis, cell migration, tissue repair and cell death (*2*). Binding of integrin to the extracellular matrix has been shown to induce various intracellular responses including increased pH levels, transient Ca^{2+} influxes, and activation of focal adhesion (*3*). Endothelial cells play a critical part in vascular homeostasis such as blood coagulation, vascular contraction, and the control of vascular permeability. In particular, endothelial cells are important in wound healing, tumor progression and metastasis because of their capacity for angiogenesis (*4*). Integrins of endothelial cells participate in regulating these physiological processes of the cells (*5*, *6*).

Snake venom metalloproteases, belonging to the metzincin family, are classified into four major groups by their protein domain structures or cDNA sequences (*7*, *8*). Class P-I enzymes consist of only the protease domain of about 25 kDa and are designated as low molecular weight metalloproteases. Class P-II enzymes consist of the protease and disintegrin domains and are known as precursor forms of disintegrins. The disintegrin domain might be released autocatalytically or by the action of another unknown protease activity (*8*, *9*). Class P-III enzymes consist of proprotein, metalloprotease, disintegrin-like and cysteine-rich domains and Class P-IV enzymes have an additional disulfide-linked C-type lectin domain. Metalloproteases from various snake venoms induce hemorrhage by digesting components of the extracellular matrix and by hydrolyzing various blood coagulation factors. Recently, snake venom metalloproteases such as HV1 (*10*, *11*), VAP-1 (*12*), graminelysin I (*13*), and agkistin (*14*) were reported to induce apoptosis of human endothelial cells. However, the molecular mechanism of this apoptosis is not clearly understood. Mammalian proteins homologous to snake venom metalloproteases are classified into a disintegrin and metalloprotease (ADAM) family. The first identified ADAM is fertilin α/β, which is known to be essential for integrin-mediated sperm-egg fertilization on the surface of sperm

[*]To whom correspondence should be addressed. Tel: +82-2-2123-2700, +82-2-362-9897, E-mail: dskim@yonsei.ac.kr

 © 2003 The Japanese Biochemical Society.

Downloaded from http://jb.oxfordjournals.org/ at Changhua Christian Hospital on September 29, 2012

cells (*15*). Several ADAMs have been implicated in many important cellular processes such as the release of tumor necrosis factor-α by ectodomain shedding (*16*), myoblast fusion (*17*), and neural development by the activation of Notch receptors (*18*).

In this study, we report the purification and cDNA cloning of a novel snake venom metalloprotease, designated as halysase, that is capable of inducing apoptosis of human umbilical vein endothelial cells (HUVECs) and suppressing the cell proliferation. Metalloprotease activity of the enzyme is able to hydrolyze not only ECM proteins but also their cell surface integrin receptors. This is the first report demonstrating that two distinct domains of halysase, the metalloprotease domain and the disintegrin-like domain, cooperatively contribute to induce apoptotic cell death of endothelial cells.

MATERIALS AND METHODS

Materials—Fresh venom of *Gloydius halys* was obtained from a local snake farm in Korea. Human fibrinogen, human type II, IV, V collagens, heparin, trypsin, Tween-20, Schiff's reagent, and bovine serum albumin (BSA) were purchased from Sigma Chemical Co. (St. Louis, MO). SDS-PAGE gel, isoelectric focusing gel, molecular weight markers, M199, gelatin, and fetal bovine serum (FBS) were purchased from Invitrogen (Carlsbad, CA). Vitronectin was obtained from TaKaRa (Shiga) and TCA from Fisher Scientific (Springfield, NJ). Human fibronectin was from Upstate Biotechnology (Lake Placid, NY). Bovine collagen Type I was obtained from Collaborative Biomedical Products (Bedford, MA). Human integrin α1β1, α5β1, αvβ3, and αvβ5 were purchased from Chemicon (Temecula, CA). Q-Sepharose fast flow, phenyl-Sepharose, Mono-Q HR 5/5 column and Superdex 75 H/R 10/30 column were products of Amersham Biosciences (Uppsala, Sweden).

Purification of Halysase—One gram of crude venom diluted with 50 ml of 20 mM Tris-HCl (pH 8.0) was loaded onto a Q-Sepharose column (2.6 × 10 cm) pre-equilibrated in the same buffer solution, sufficiently washed with the buffer, and then eluted with the buffer containing 50 mM NaCl. Metalloprotease activity was assayed by analyzing the degradation pattern of fibrinogen and by observing the induction of HUVEC apoptosis. Active fractions were pooled, concentrated and separated in a Superdex 75 HR 10/30 gel filtration column (1 × 30 cm) equilibrated with PBS. Fractions that hydrolyze fibrinogen were collected and dialyzed against 20 mM Tris-HCl (pH 8.0). Dialyzed sample was loaded onto a Mono-Q HR 5/5 column (0.5 × 5 cm) equilibrated in 20 mM Tris-HCl (pH 8.0), then eluted with a linear gradient of 0–1 M NaCl. The purified metalloprotease, named halysase, was analyzed by SDS-PAGE and isoelectric focusing.

Characterization of Halysase—N-terminal and internal amino acid sequences of halysase were determined by Edman degradation with protein sequencer (PE Applied Biosystems, Foster City, CA). To analyze the internal amino acid sequences of the protein, 7.5 μM purified halysase was partially digested with 0.1 nM trypsin for 3 h in 20 mM Tris-HCl (pH 8.0) buffer containing 150 mM NaCl and 5 mM $CaCl_2$. Purified halysase and trypsinized halysase were subjected to SDS-PAGE, then electrotransferred to PVDF membrane (Bio-Rad, Hercules, CA). The protein bands were analyzed with a protein sequencer. PAS staining was carried out as previously described (*19*). To deglycosylate the protein, 1.5 μM of denatured halysase was incubated with 0.25 unit of *N*-glycosidase F (Roche Applied Science, Mannheim, Germany) for 24 h at 37°C in 20 mM sodium phosphate (pH 7.5). Deglycosylated halysase was examined by PAS staining on SDS-PAGE.

cDNA Cloning of Halysase—The cDNA library of *Gloydius halys* venom gland was constructed following the protocols of the λZAP™XR cDNA cloning kit (Stratagene, La Jolla, CA) and an *in vitro* packaging kit (Amersham Biosciences) as described in our previous report (*20*). A degenerated forward primer 5′-TC(A/G/T/C)CA(A/G)TC (A/G/T/C)AA(T/C)CTTACTCC-3′ and reverse primer 5′-CC(A/G)TT(A/G)TA(A/G)CA(A/G)TA(A/G/T/C)CC(A/G)TT-3′ were designed according to the determined N-terminal amino acid sequence and internal sequence of halysase. The polymerase chain reaction (PCR) was performed with the designed primers and the PCR product was subcloned into pGEM-T Easy vector (Promega, Madison, WI). The sequence of the subcloned fragment was determined with an ABI PRISM Dye Sequencing Kit (PE Applied Biosystems). To obtain full-length cDNA of the halysase, the rapid amplification of cDNA ends (RACE) PCR was carried out with gene-specific primers designed on the basis of the PCR fragment sequence. For the 5′ region of the cDNA, the PCR was performed with a gene-specific antisense primer (5′-CGCCCAAGTAACCAAGT-CCTGC-3′) and SK primer. To obtain the 3′ region of the cDNA, PCR was performed with a specific sense primer (5′-GGAGGTGGGAGAAGATTGTGACTGTGGC-3′) and T7 primer. The full-length cDNA sequence and the deduced amino sequence of halysase were compared in the GenBank Swiss-Prot by using the BLAST search program.

Cloning, Expression, and Purification of the Disintegrin-Like Domain—The cDNA encoding the disintegrin-like domain was cloned from the cDNA of halysase by PCR as described in our previous report (*21*). The amplified cDNA of the disintegrin-like domain was transferred into *Pichia pastoris* expression vector, pPIC9 (Invitrogen). The pPIC9-disintegrin-like domain vector was digested with *Sal*I (NEB, Beverly, MA) restriction enzyme. This linearized plasmid was transformed into electro-competent GS115 cells (Gene Pulser, Bio-Rad). Stock *P. pastoris* cells were grown at 30°C in 250 ml of glycerol minimal medium. After 24 h, cells were collected by centrifugation and transferred into 500 ml of methanol minimal medium. A total of 0.5% methanol was added every 24 h to induce recombinant protein expression for 2 days. Ammonium sulfate was added to the collected supernatant to reach 2 M, and the resulting solution was loaded onto a phenyl-Sepharose column followed by protein elution with a gradient of 2–0 M ammonium sulfate. The disintegrin-like domain expressed by *P. pastoris* was further purified by Q-Sepharose ion-exchange chromatography and Superdex 75 gel filtration chromatography. Newly induced recombinant protein corresponding to 8 kDa was monitored by SDS-PAGE analysis throughout the purification procedure. N-terminal sequencing analysis of the recombinant disintegrin-like domain was per-

Downloaded from http://jb.oxfordjournals.org/ at Changhua Christian Hospital on September 29, 2012

formed by automated Edman degradation procedure, and the obtained sequence was compared with the cDNA-deduced polypeptide sequence.

Enzyme Activity of Halysase—Fibrinolytic activity was measured according to the pervious method (*22*). Human fibrinogen (10 μg) was incubated with 15 nM purified halysase or apohalysase in 20 mM Tris-HCl (pH 8.0) containing 150 mM NaCl and 1 mM $CaCl_2$ at 37°C for 2 h. Apohalysase was prepared by pre-incubating halysase with 10 mM EDTA in 20 mM Tris-HCl (pH 7.5) for 24 h at 4°C. Then the reaction buffer was changed three times with 20 mM Tris-HCl (pH 7.5) using Microcon-10 (Millipore, Bedford, MA). Each ECM protein (2.5 × 5 μg), including vitronectin, fibronectin, collagen type I, II, IV, and V, was incubated with 75 nM halysase or apohalysase in 20 mM Tris-HCl (pH 8.0) containing 150 mM NaCl and 1 mM $CaCl_2$. The enzyme reaction was allowed to proceed for 16 h at 37°C. Human integrins (3 μg each) were also reacted with 45 nM halysase under the same conditions. The proteolytic reaction products were analyzed by SDS-PAGE.

Cell Culture—HUVECs were cultured as previously described (*23*). The cells were maintained on gelatin-coated plastic dishes (Nunc, Roskilde, Denmark) in M199 culture media containing 20% (v/v) heat-inactivated FBS, 10 units/ml of heparin, 3 ng/ml of bFGF (Upstate Biotechnology), and 1% (v/v) antibiotics. The endothelial cells used in all experiments were from passages 3–5.

HUVEC Proliferation, Adhesion, and Tube Formation—HUVEC proliferation assay was performed by measuring incorporated [^{3}H]thymidine (NEN, Boston, MA) (*24*). HUVECs (2.5×10^4 cells/ ml) were incubated onto gelatin-coated 48-well culture plates (0.25 ml/well) in complete medium with 5% CO_2 for 24 h at 37°C. After starvation in the basal media containing 1% FBS for 6 h, the cells were cultured with the complete media containing each protein sample (2.5–20 nM) for 30 min, then treated with 3 ng/ml bFGF. Following an additional 3-h incubation, the cells were pulsed with 1 μCi of [^{3}H] hymidine for 9 h and washed twice with PBS on ice. The cells were fixed with 3% (v/v) formaldehyde at 4°C for 5 min and washed twice with PBS. Then, 5% (w/v) TCA was added, and incubation was continued for 15 min at 4°C. After washing twice with PBS, the acid-insoluble precipitate was dissolved in 0.3 N NaOH for 30 min, then radioactivity was measured with a liquid scintillation counter (Perkin-Elmer Life Science, Boston, MA).

HUVEC adhesion assay was performed with modified method as previously described (*25*). Culture plates (96-well) were coated with 1 μg/well of several ECM proteins for 16 h at 4°C. The plates were washed and incubated with 1% (w/v) BSA for 2 h at 37°C. HUVECs (2×10^5 cells/ ml) were pre-incubated with 75 nM of halysase or salmosin (*25*) for 30 min at 37°C. After washing the plates with PBS, the cell suspension (0.1 ml) was added to each coated well and incubated for 1 h at 37°C. Unattached cells were then removed by washing with PBS. Attached cells were fixed and stained with Coomassie blue R. Absorbance at 540 nm was measured for individual wells to determine the relative number of cells. Data were expressed as the mean ± SEM from three separate experiments. Tube formation of the endothelial cells was performed as previously described (*26*). A 24-well culture plate was coated with 0.25 ml/well of Matrigel (BD, Franklin Lakes, NJ) solution, then incubated at 37°C for 1 h to allow gel formation. HUVECs (4×10^4 cells/well) were seeded on Matrigel with 5 ng/ml bFGF in the presence or absence of 15 nM halysase, incubated at 37°C for 24 h, then photographed.

Analysis of HUVEC Apoptosis—HUVECs were grown on gelatin-coated 24-well culture plates until the cells reached 70–80% of confluence. In fresh media, the cells were incubated with 10 nM of each protein sample for 24 h at 37°C. Then, the cells were sequentially stained with 10 μM Hoechst 33258 (Sigma) for 30 min and propidium iodide (Sigma) for 5 min. Nuclear fragmentation was examined by inverted fluorescence microscopy (Carl Zeiss, Jena, Germany).

Caspase-3 activity was determined colorimetrically using a CaspACE Assay System (Promega). HUVECs were grown on gelatin-coated 60-mm culture dishes. The cells were incubated for 3–9 h with 10 nM halysase, harvested by scraping and centrifugation at 4°C, then lysed in the lysis buffer by freezing and thawing. Caspase-3 assay was performed with the cell lysate in a 96-well plate according to the manufacturer's instructions. To detect the activated caspase-3 and cleaved PARP, a major substrate of caspase-3, in the cell lysate, Western blot analysis was carried out. The cell lysate (30 μg) was subjected to SDS-PAGE, and transferred onto NC membrane. After blocking the transferred membrane with PBS containing 0.05% (v/v) Tween-20 and 5% (w/v) skim milk (Difco, Sparks, MD), it was incubated with anti-cleaved caspase-3 antibody (Cell Signaling, Beverly, MA) or anti-cleaved PARP antibody (Chemicon) for 2 h. The membrane was washed four times with 0.05% Tween-20 in PBS for 20 min, then incubated for 2 h with goat anti-rabbit Ig G conjugated to horse-radish peroxidase (Accurate, Westbury, NY). After extensive washing, the immune complex was visualized using chemiluminescence (Amersham Biosciences).

Analysis of Apoptosis-Regulating Proteins—In the lysate of halysase-induced apoptotic endothelial cells, apoptosis-regulating proteins were analyzed by Western blot assay. An anti-Bcl-2 polyclonal antibody, anti-Bcl-X_L poly-

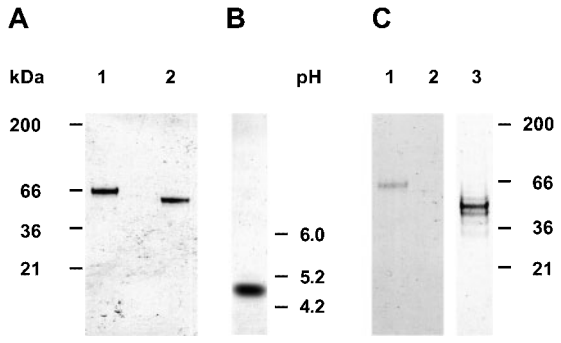

Fig. 1. **SDS-PAGE of purified halysase.** (A) Purified halysase was analyzed in 4–20% gradient SDS-PAGE under reducing conditions (lane 1) and non-reducing conditions (lane 2). (B) Isoelectric focusing of halysase in the range of pH 3–10. (C) Carbohydrate staining of halysase (lane 1) and deglycosylated halysase (lane 2) with PAS reagent in SDS gel. Halysase was deglycosylated with N-glycosidase as described in "MATERIALS AND METHODS." Deglycosylated halysase was stained with CoomassieBblue (lane 3).

Downloaded from http://jb.oxfordjournals.org/ at Changhua Christian Hospital on September 29, 2012

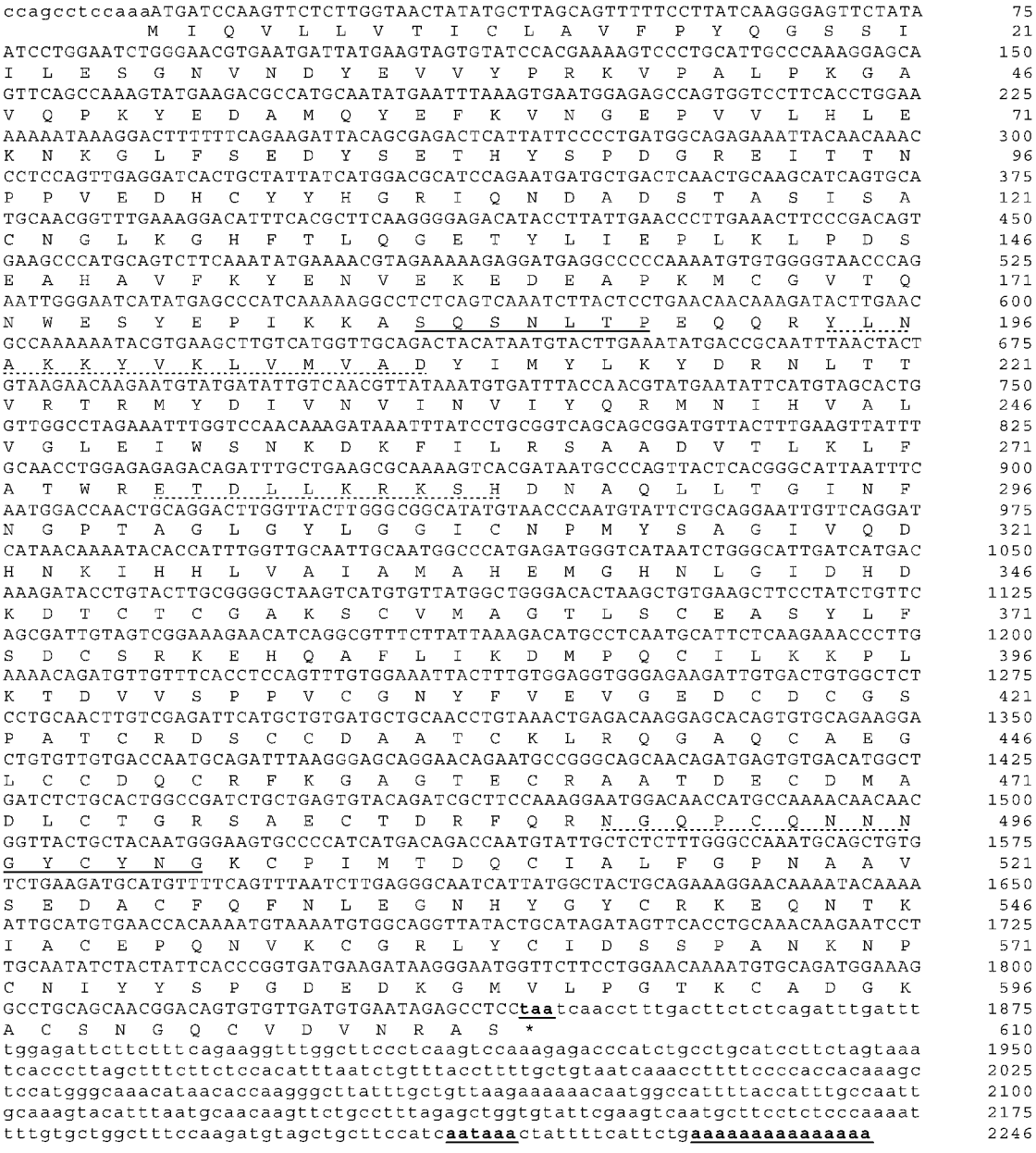

Fig. 2. **cDNA and deduced amino acid sequences of halysase.** cDNA coding regions are shown in capital letters, and the 5′- and 3′-untranslated regions in small letters. The deduced amino acid sequence is denoted by one-letter symbols. Degenerated primers for the cDNA cloning were designed on the basis of the underlined amino acid sequences determined by Edman degradation. Internal amino acid sequences of trypsinized halysase determined by protein sequence analysis are shown by dotted underline. Termination codon and polyadenylation signal are underlined in bold-faced small letters.

clonal antibody, anti-Bad polyclonal antibody (Santacruz Biotechnology, Santacruz, CA), and anti-Bax polyclonal antibody (Delta Biolabs, Campbell, CA) were used in Western blot analysis with anti-α-tubulin polyclonal antibody (Accurate) as a control.

RESULTS

Purification and Characterization of Halysase—A novel hemorrhagic metalloprotease was isolated from the snake venom of *Gloydius halys* and designated as halysase. The crude venom was initially fractionated by anion-exchange chromatography in a column of Q-Sepharose. The active fractions recovered in 50 mM NaCl were assayed by monitoring degradation of fibrinogen as well as induction of endothelial cell death. Superdex 75 gel filtration and Mono-Q anion-exchange chromatography were performed for further purification. Purified halysase showed an apparent molecular mass of 66 kDa on SDS-PAGE analysis under reducing conditions (Fig. 1A, lane 1). The protein migration pattern of the purified enzyme in SDS-PAGE was slightly different depending on whether or not the polypeptide chain was reduced (Fig. 1A). Such a difference in protein mobility may be due to the physical properties of the polypeptide chain bearing multiple disulfide bonds.

Downloaded from http://jb.oxfordjournals.org/ at Changhua Christian Hospital on September 29, 2012

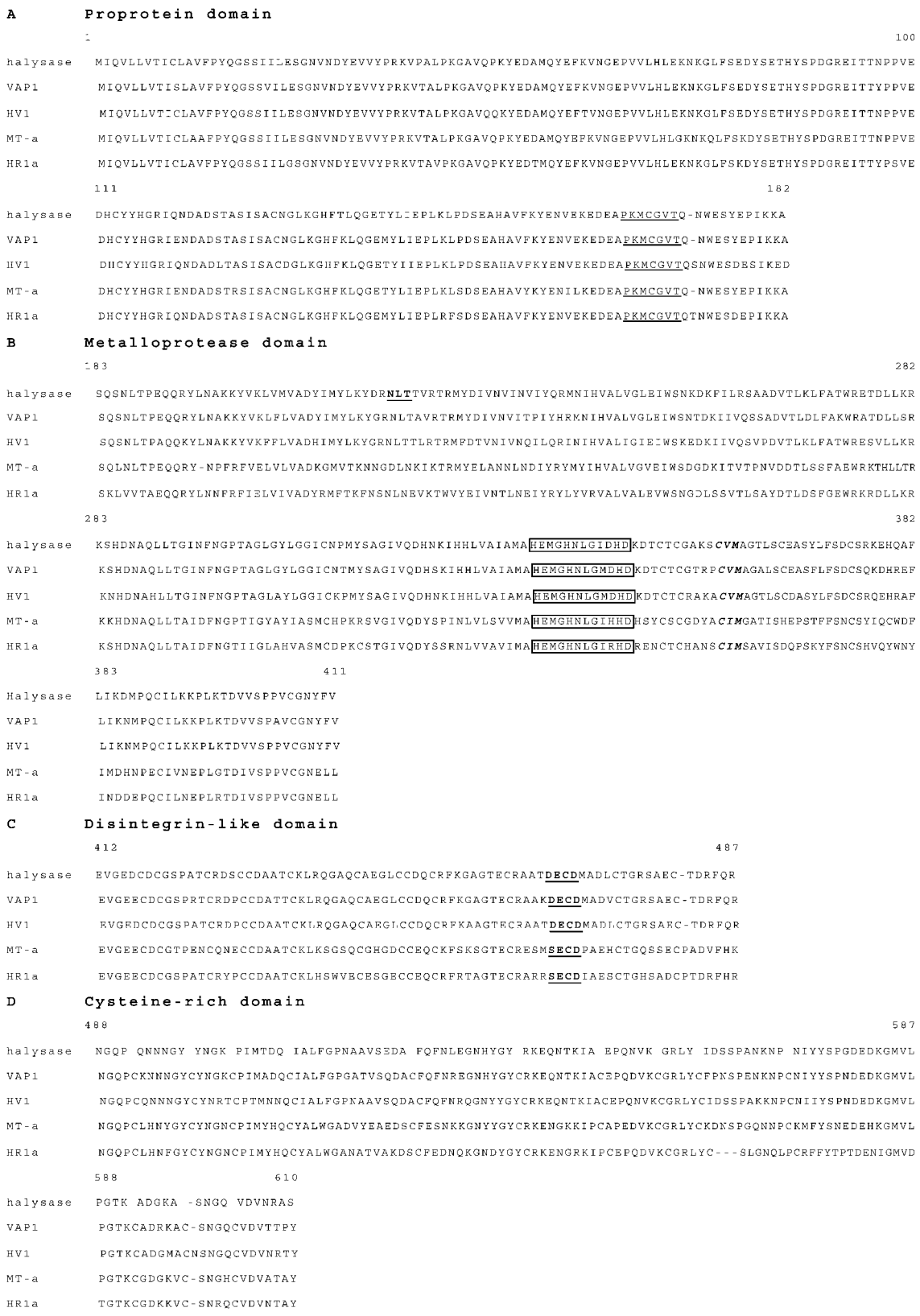

Fig. 3. **Comparison of deduced amino acid sequences.** Deduced amino acid sequence of halysase is aligned with that of other snake venom metalloproteases. The GenBank accession numbers of the cDNA sequences of HR1a and MT-a are AB074143 and AF051787, respectively. In the proprotein domain (A), the cysteine switch motifs are underlined. In the metalloprotease domain (B), the consensus sequence of zinc-binding site of MDC or ADAM proteins is boxed, and the methionine-turn region is shown in italics. The putative glycosylation sites of halysase are underlined. In the disintegrin-like domain (C), the DECD or SECD sequence that is recognized by integrin receptor is underlined. In the cysteine-rich domain (D), conserved cysteine residues are shown by dots.

Downloaded from http://jb.oxfordjournals.org/ at Changhua Christian Hospital on September 29, 2012

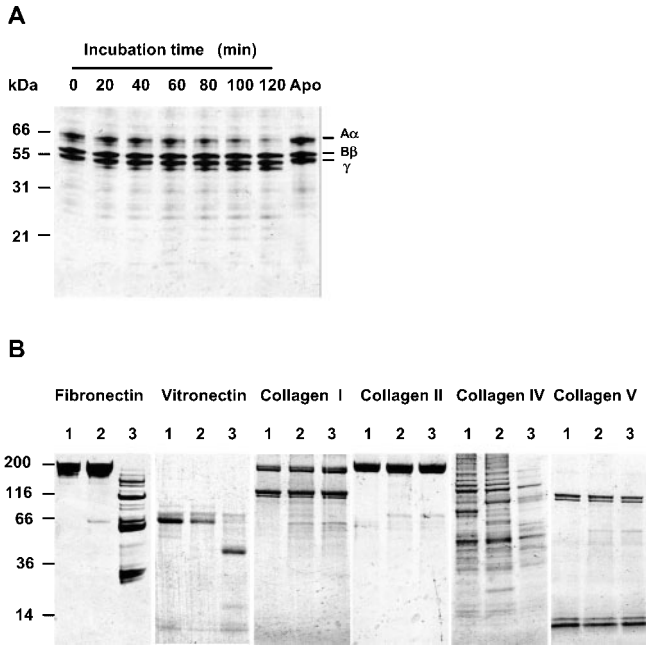

Fig. 4. **Proteolytic degradation of fibrinogen and ECM proteins by halysase.** Fibrinogen (A) and ECM proteins (B) were incubated with or without halysase, and then analyzed by 4–20% gradient SDS-PAGE under reducing conditions. Fibrinogen was reacted with halysase for 0–120 min at 37°C in 20 mM Tris-HCl (pH 8.0) containing 150 mM NaCl and 1 mM $CaCl_2$. As a control, fibrinogen was incubated for 120 min under the same conditions with apohalysase prepared by EDTA treatment (Apo). Several ECM proteins (lanes 1) were incubated with apohalysase (lanes 2) or halysase (lanes 3) for 16 h under the same conditions as described above.

Isoelectric focusing analysis revealed that halysase is a rather acidic protein with a pI of 4.8 (Fig. 1B). PAS staining result indicated that the purified halysase is a glycoprotein (Fig. 1C, lane 1). When the covalently attached carbohydrate structures were removed from halysase by N-glycosidase treatment, the protein band that gives negative reaction with PAS (Fig. 1C, lane 2) migrated as a smaller molecular size, corresponding to 47 kDa, than its native form (Fig. 1C, lane 3).

cDNA Cloning of Halysase—Molecular cloning of cDNA encoding halysase was carried out with oligonucleotide primers designed on the basis of the N-terminal and internal amino acid sequences of the protein as described in Materials and Methods. Sequence analysis revealed that the cDNA clone consists of 2,246 bases including a 5′-end non-translating region of 12 nucleotides, an open reading frame of 1,833 nucleotides, and a 3′-end non-translating region of 401 nucleotides containing the termination codon AATAAA and a polyadenylation site (Fig. 2). Based on the deduced polypeptide sequence, the open reading frame of the cDNA is composed of 610 amino acids, corresponding to the calculated molecular mass of 67.65 kDa. A signal sequence of 18 amino acids was found in the N-terminal region of the deduced polypeptide sequence. The signal sequence was followed by a proprotein domain, a metalloprotease domain, a disintegrin-like domain and a cysteine-rich domain. The N-terminal sequence determined directly by Edman degradation indicated that the purified halysase polypeptide chain is devoid of the proprotein domain.

A search of the GenBank database revealed that halysase has strong sequence similarity with other members of the apoptosis-inducing snake venom metalloprotease/disintegrin/cysteine-rich (MDC) family, such as HV1 from *Trimeresurus flavorviridis* (*11*) and VAP1 from *Crotalus atrox* (*12*). Sequence homologies of halysase with HV1 and VAP1 were 87% and 88%, respectively (Fig. 3). The cysteine switch motif, PKMCGVT, was conserved in the proprotein domain (Fig. 3A) and the characteristic zinc-chelating sequence of MDC or ADAM protein, HEXXHXXGXXHD, was found in the protease domain of halysase (Fig. 3B). Residues His285, Gln289, and Ile294, which are generally conserved in hemorrhagic proteases, may be responsible for binding of the metalloprotease to the basement membrane (*27*). However, the methionine-turn CIM, which is involved in zinc-binding (*28*), was replaced by CVM in the protease domain of halysase. The disintegrin-like domain of halysase contained a DECD sequence in place of the RGD sequence (Fig. 3C).

Enzyme Activity of Halysase—Most snake venom metalloproteases, whether hemorrhagic or non-hemorrhagic, hydrolyze fibrinogen. The fibrinogenolytic activity of halysase was investigated by reacting the enzyme with human fibrinogen at 37°C. When the enzyme reaction products were analyzed on SDS-PAGE, halysase was able to completely degrade the fibrinogen Aα chain in 2 h without significant enzymatic cleavage of β and γ chains (Fig. 4A). Proteolytic activity of halysase was also examined with several ECM proteins. Type IV collagen, fibronectin and vitronectin were good substrates for halysase reaction, whereas the enzyme could not degrade types I, II, and V collagens (Fig. 4B). However, the catalytic activity was completely lost by pre-treatment of the enzyme with metal chelating agent such as EDTA (Fig. 4). When apohalysase was stored in a buffer solution containing 2.5 mM $CaCl_2$ and 1 mM $ZnCl_2$, the apoenzyme failed to regain its catalytic activity to hydrolyze fibrinogen (data not shown).

HUVEC Proliferation, Tube Formation, and Adhesion—To examine the functional properties of halysase at the cellular level, HUVEC proliferation was observed by measuring thymidine incorporation in the presence or absence of the enzyme. Figure 5A shows that halysase retains potent activity to inhibit the endothelial cell proliferation in a dose-dependent manner. HUVEC proliferation is well known to be highly stimulated by bFGF treatment (*29*). In this bFGF-induced HUVEC proliferation system, intracellular DNA synthesis was significantly reduced in the presence of halysase. Interestingly, however, apohalysase, which is devoid of metal ions in its metalloprotease domain, was also able to inhibit the proliferation to about 50% of the extent of inhibition by native enzyme. These experimental results demonstrate that the proteolytic activity of halysase is partly associated with the inhibition of endothelial cell proliferation. It is also conceivable that another functional domain such as the disintegrin-like domain may be involved in the suppressed proliferation. To clarify the functional role of the independent disintegrin-like domain (Fig. 3C), cDNA encoding the domain was cloned and expressed in

Downloaded from http://jb.oxfordjournals.org/ at Changhua Christian Hospital on September 29, 2012

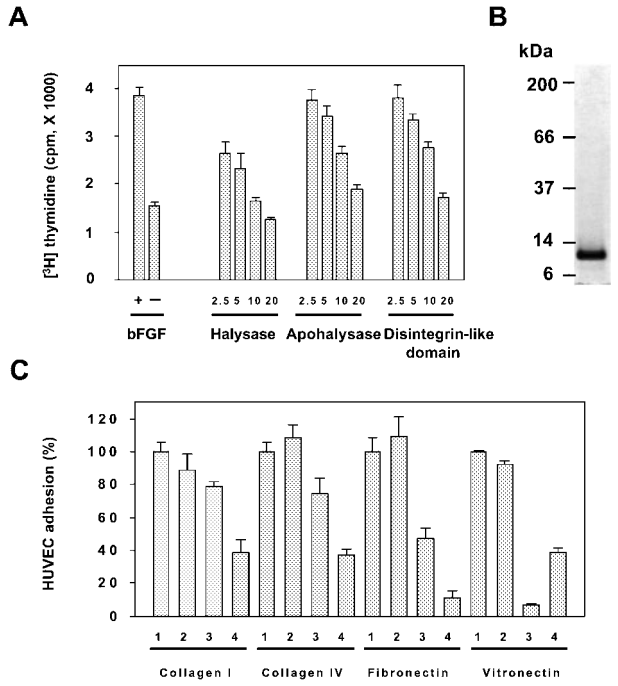

Fig. 5. **Inhibition of bFGF-induced HUVEC proliferation and adhesion.** (A) HUVECs (6.25×10^3 cells) were pretreated with 2.5–20 nM protein sample for 3 h at 37°C in the presence of 3 ng/ml bFGF, then incubated with 1 μCi [^{3}H]thymidine for 9 h, followed by radioactivity measurement in liquid scintillation counter. As a control, the cells were pretreated with 3 ng/ml bFGF alone. (B) The disintegrin-like domain of halysase was expressed in *Pichia pastoris*. Purified recombinant protein was analyzed by 4–20% gradient SDS-PAGE. (C) ECM proteins were immobilized onto a 96-well plate, then incubated for 1 h with HUVECs (2×10^4 cells) pretreated with PBS (1), BSA (2), salmosin (3), and halysase (4). Attached cell numbers were measured as described in "MATERIALS AND METHODS."

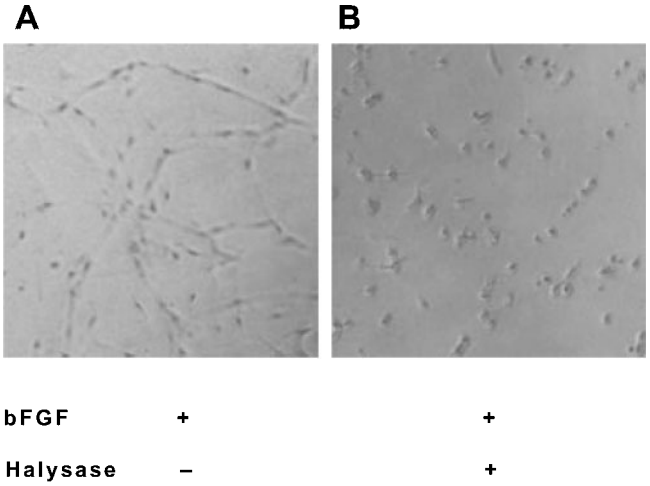

Fig. 6. **Inhibition of bFGF-induced HUVEC tube formation.** HUVECs (4×10^4 cells) were grown for 24 h at 37°C on Matrigel containing 5 ng/ml of bFGF in the absence (A) or presence (B) of 15 nM halysase, followed by microscopic observation.

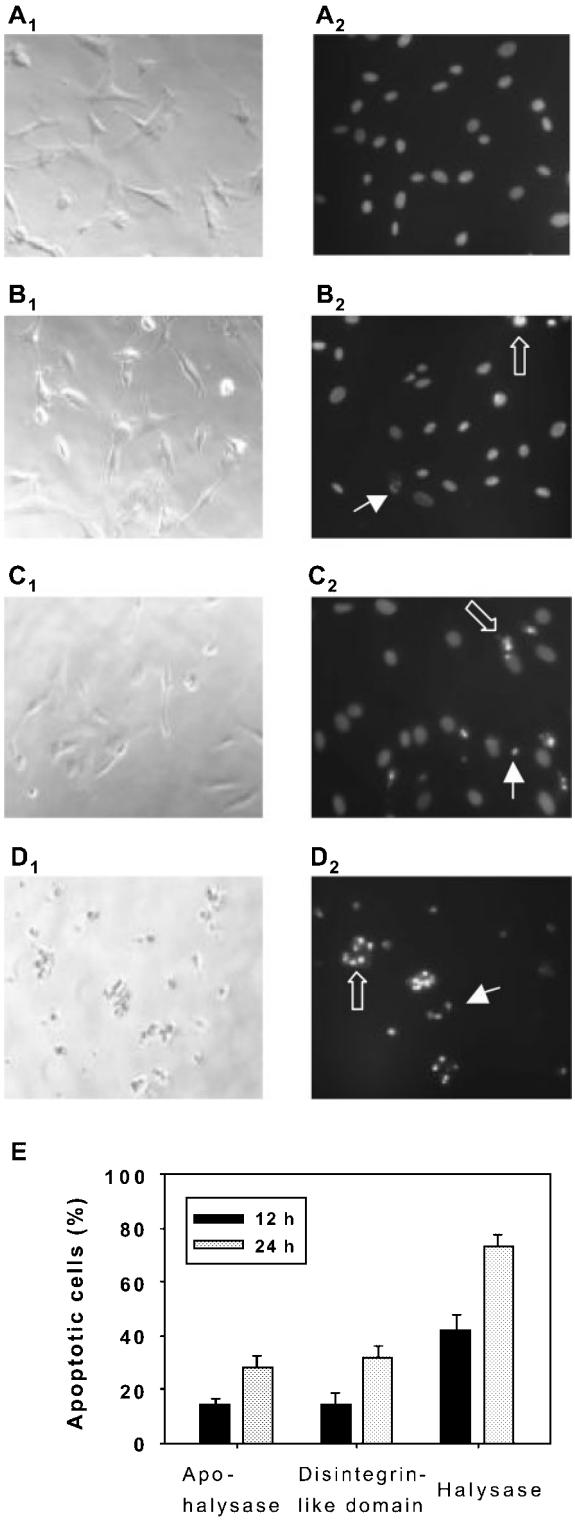

Fig. 7. **Induction of HUVEC apoptosis by halysase.** HUVEC apoptosis was observed under a light microscope (A_1–D_1) and an inverted fluorescence microscope (A_2–D_2). HUVECs were cultured for 24 h at 37°C on gelatin-coated culture plate (A_1, A_2) with 10 nM apohalysase (B_1, B_2), recombinant disintegrin-like protein (C_1, C_2) or halysase (D_1, D_2). Samples were stained with 10 μM Hoechst 33258 and propidium iodide (A_2–D_2). Open and closed arrows indicate apoptotic cells stained with Hoechst 33258 and propidium iodide, respectively. The percentage of apoptotic endothelial cells (E) was measured in randomly selected microscopic fields.

Downloaded from http://jb.oxfordjournals.org/ at Changhua Christian Hospital on September 29, 2012

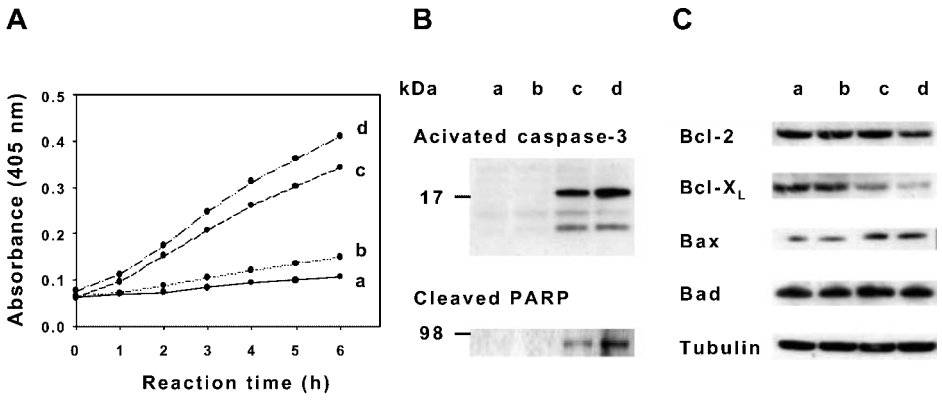

Fig. 8. **Caspase-3 assay and analysis of apoptosis-regulating proteins in apoptotic HUVEC.** HUVECs were treated with PBS at 37°C for 9 h as a control (a). The cells were incubated with 10 nM halysase for 3 h (b), 6 h (c), and 9 h (d). Caspase-3 activity in the cell lysate was measured by colorimetric assay (A). Activated caspase-3 and cleaved PARP were examined by Western blot (B). Levels of Bcl-2 family proteins were also estimated by Western blot analysis (C). (A) The cell lysate was reacted at 37°C with chromogenic substrate, Ac-DEVD-*p*-nitroanilide for 6 h, and absorbance 405 nm was measured during the reaction. (B) The cell lysate was subjected to SDS-PAGE, and the activated caspase-3 and cleaved PARP were identified with the anti-cleaved caspase-3 antibody and the anti-cleaved PARP antibody, respectively. (C) Bcl-2 family proteins in the cell lysate were analyzed by SDS-PAGE with their corresponding antibodies as described in "MATERIALS AND METHODS."

Pichia pastoris (Fig. 5B). The recombinant disintegrin-like protein containing a DECD sequence in the putative integrin-binding motif was also able to inhibit the bFGF-induced HUVEC proliferation in a dose-dependent manner, and its inhibitory activity was comparable to that of apohalysase (Fig. 5A).

To investigate the functional characteristics of the disintegrin-like domain in halysase, endothelial cell adhesion assay was performed with several ECM proteins (Fig. 5C). As evidenced in our previous report (*25*), RGD-containing disintegrin, salmosin, significantly suppresses the cell adhesion to vitronectin. Unlike salmosin, halysase remarkably inhibited adhesion of the endothelial cells to fibronectin. These results imply that the disintegrin-like domain of halysase interacts more strongly with β1-containing integrins than with other integrin species on the cell surface. The functional role of halysase was further examined by carrying out tube formation assay of HUVECs in Matrigel in the presence or absence of the protein. Formation of a 3-dimensional network structure of the cells induced by proliferation and migration can be visualized in the assay system (*26*). As illustrated in Fig. 6, halysase strongly suppressed bFGF-stimulated tube formation of HUVECs in Matrigel containing various ECM proteins.

Induction of HUVEC Apoptosis—Based on the experimental results indicating that halysase inhibits HUVEC proliferation, the endothelial cells were initially observed under light microscope in the presence or absence of each protein sample (Fig. 7). The endothelial cells incubated with apohalysase, recombinant disintegrin-like domain, and halysase generated apoptotic bodies as well as floating cells with typical changes in morphology including cell shrinkage and formation of blebs on the cell surface (Fig. 7, B_1, C_1, and D_1). Analysis of cells stained with Hoechst 33258 and propidium iodide under fluorescence microscope also exhibited nuclear fragmentation of apoptotic endothelial cells (Fig. 7, B_2, C_2, and D_2). A quantitative analysis by counting the number of apoptotic cells revealed that both apohalysase and the recombinant disintegrin-like domain are much less potent inducers of apoptosis than native halysase (Fig. 7E). These results are consistent with the previous experimental observation that the proteolytic activity of halysase partly contributes to the inhibition of cell proliferation (Fig. 5A). Staining of fragmented DNA in the apoptotic cells with propidium iodide indicated that the plasma membrane of the endothelial cell was destroyed (Fig. 7, closed arrows). DNA staining of the cells with Hoechst 33258, a membrane-permeable dye, demonstrated that cells in the initial stage of apoptosis retained an intact plasma membrane (Fig. 7, open arrows).

Analysis of Caspase-3 Activation and Apoptosis Regulating Proteins—In an attempt to get more information about halysase-induced HUVEC apoptosis, caspase-3 activity was monitored with a colorimetric substrate, Ac-DEVD-*p*-nitroanilide. When the cells were treated with halysase, caspase-3 activity gradually increased with incubation time (Fig. 8A). The activated caspase-3 was also confirmed by Western blot analysis using a specific antibody against it (Fig. 8B, lanes c and d). PARP, a 116-kDa poly ADP-ribose polymerase, is a nuclear enzyme implicated in the apoptosis response. This protein, which is one of the main *in vivo* cleavage substrates of activated caspase-3, is cleaved into two fragments, an N-terminal 24-kDa fragment and a C-terminal 89-kDa catalytic domain. The cleaved 89-kDa PARP fragment also increased with the incubation time (Fig. 8B, lanes c and d). Experimental results suggest that halysase-induced apoptosis of endothelial cells is mediated by caspase-3, one of the key regulators of apoptosis.

Alterations in the level of Bcl-2 family proteins that regulate apoptosis (*30*) were examined by Western blot analysis in the endothelial cells treated with halysase (Fig. 8C). Among the anti-apoptotic Bcl-2 family proteins, Bcl-X_L decreased remarkably in the apoptotic HUVECs as incubation time with halysase increased, while Bax was increased during the apoptosis. However, the levels of Bcl-2 and Bad were not affected in halysase-induced apoptosis of the endothelial cells. Taken together, these results suggest that the characteristic apoptotic event of HUVEC induced by halysase is principally associated with down-regulation of Bcl-X_L and decreased level of Bcl-X_L/Bax.

Degradation of Integrins by Halysase—To further explore the metalloprotease activity, several types of integrins were reacted with halysase *in vitro*, then the enzyme activity was analyzed by SDS-PAGE. Proteolytic

Downloaded from http://jb.oxfordjournals.org/ at Changhua Christian Hospital on September 29, 2012

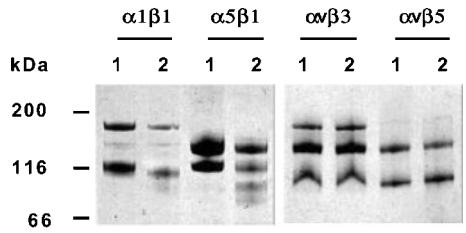

Fig. 9. **Degradation of integrins by halysase.** Each human integrin (lanes 1) was reacted with halysase (lanes 2) at 37°C for 16 h in 20 mM Tris-HCl (pH 8.0) containing 150 mM NaCl and 1 mM $CaCl_2$. Proteolytic degradation of the integrins was examined by SDS-PAGE.

activity of halysase was able to degrade integrins α1β1 and α5β1, but not integrins αvβ3 and αvβ5 (Fig. 9, lanes 2). It is interesting to note that integrins composed of β1 subunit were more susceptible to the enzymatic hydrolysis than other types of integrins. These observations are correlated with those of the adhesion assay, suggesting that halysase more strongly inhibits the endothelial cell adhesion to fibronectin that binds to integrin α5β1 on the cell surface than to other ECM proteins. It has been reported that not only integrin αvβ3 but also β1-containing integrins such as integrin α2β1 and α5β1 play an important role in anchorage-dependent cell survival (*31*, *32*). In halysase-induced apoptosis of endothelial cells, proteolytic degradation of integrins may result in dysfunction of integrins on the cell surface, which are closely associated with apoptosis.

DISCUSSION

The biochemical and physiological significance of functionally distinct protein modules such as the disintegrin-like domain and the metalloprotease domain of MDC or ADAM proteins has not yet been elucidated. In the case of snake venom metalloprotease, it was suggested that the two distinct protein domains are autoproteolysed from the precursor during venom collection and protein purification (*8*, *9*). We also proposed in our previous report that the disintegrin domain in a snake venom metalloprotease modulates the catalytic function of the enzyme in hydrolyzing extracellular matrix proteins (*20*).

In this work, we report the purification and cDNA cloning of a novel snake venom metalloprotease, halysase, from *Gloydius halys*. The deduced amino acid sequence from the cDNA encoding halysase revealed that the metalloprotease has multifunctional domains including a proprotein domain, a protease domain, a disintegrin-like domain and a cysteine-rich domain. Since halysase has 35 cysteines, the different mobilities of the enzyme on SDS-PAGE under reducing and non-reducing conditions may be due to the presence of multiple intrachain disulfide bridges of the polypeptide chain (Fig. 1A, lane 1 and 2). Although the estimated molecular mass of halysase, a glycoprotein, was 66 kDa in SDS-PAGE analysis (Fig. 1A, lane1), the deglycosylated polypeptide size was determined to be 47 kDa (Fig. 1C, lane 3) which is consistent with the calculated mass of the deduced sequence. As indicated in Fig. 3, there is a putative glycosylation site, N^{218}-L-T^{220}, in the halysase polypeptide chain.

Since native halysase and apohalysase exhibited distinct potencies in suppressing DNA synthesis of HUVECs (Fig. 5A), it is evident that the catalytic function of halysase is associated with proliferation of the cell. However, it has to be considered that the metalloprotease activity of halysase is not the only element responsible for the suppressed proliferation, because apohalysase was also able to significantly inhibit the proliferation. It is reasonable to speculate that the observed residual activity of apohalysase to inhibit the cell proliferation might be due to the disintegrin-like domain of the enzyme. This was further supported by the experimental evidence showing that the recombinant disintegrin-like domain inhibits the endothelial cell proliferation with comparable potency to the apohalysase (Fig. 5A). In most anchorage-dependent cells, cellular processes such as proliferation and migration are mediated by various integrins on the cell surface. Therefore, it is possible to suggest that the disintegrin-like domain of halysase plays an important role in inhibiting the endothelial cell adhesion to ECM proteins or tube formation of the cells (Figs. 5C and 6). Similar results obtained with a typical snake venom disintegrin, salmosin (*25*), strongly support the functional significance of the disintegrin-like domain of halysase. It is well known that the disintegrins interact with diverse integrin species (*33*, *34*). Like salmosin, disintegrins containing the RGD sequence have been reported to inhibit proliferation and migration of endothelial cells (*25*, *35*) and smooth muscle cells (*36*) by interacting with integrin αvβ3, which is a major receptor for vitronectin. On the other hand, the disintegrin-like domain of halysase containing the DECD sequence in place of RGD sequence appears to interact with integrins containing the β1 subunit, such as α5β1, which is a major receptor for fibronectin. There is a report indicating that a snake venom metalloprotease, jararhagin, containing the SECD sequence in its disintegrin-like domain inhibits platelet aggregation by interacting with α2β1 integrin, which is expressed on the platelet surface (*37*, *38*).

Snake venom metalloproteases, which are composed of multifunctional domains, have been reported to induce the endothelial cell apoptosis (*10–12*, *14*). However, little information is available to explain the biochemical mechanism of the metalloprotease-induced apoptotic event. As demonstrated in proliferation experiments (Fig. 5A) in this work, both metalloprotease activity and the disintegrin-like domain of halysase contribute to the induction of HUVEC apoptosis (Fig. 7). Metalloprotease activity of halysase is capable of preferentially degrading ECM proteins including type IV collagen, fibronectin and vitronectin (Fig. 4). Such a substrate specificity of the enzyme might be closely related to the induction of the endothelial cell apoptosis. It is generally accepted that ECM proteins play critical roles in organizing the structure and function of the matrix (*39*). Several ECM proteins have been shown to specifically interact with one another and with anchorage-dependent cells (*39*). Proteolytic degradation of one or more of these proteins may lead to the destruction of structural integrity of ECM, resulting in functional disruption. When anchorage-dependent cells

Downloaded from http://jb.oxfordjournals.org/ at Changhua Christian Hospital on September 29, 2012

including epithelial and endothelial cells are detached, they undergo apoptosis, so called anoikis (*40*, *41*). Based on our experimental evidence, it is postulated that enzyme activity of halysase induces the endothelial cell apoptosis by degrading not only ECM proteins but also cell-surface integrins, leading to the cell detachment. It was demonstrated in a previous report that antibodies against α3, α6, and β1 were able to inhibit the metalloprotease-induced apoptosis of endothelial cells (*42*). It is also meaningful to hypothesize that the disintegrin-like domain of halysase is able to target the enzyme to the cell-surface integrins. The metalloprotease domain of the enzyme then exerts its catalytic function on the suitable substrates including integrins and ECM proteins. Several lines of experimental evidence suggest that the metalloprotease domain and the disintegrin-like domain of halysase cooperatively contribute to the endothelial cell apoptosis. Halysase-induced apoptosis of endothelial cells was found to be mediated by the activation of caspase-3, and the particular apoptotic event was characterized by a decreased level of Bcl-X_L and an increased level of Bax among Bcl-2 family proteins. The Bcl-2 family proteins are involved in regulation of apoptosis induced by various cellular signals. Members of the Bcl-2 family share some structural homology, but function either to promote (pro-apoptotic) or inhibit (anti-apoptotic) cell death (*30*, *32*). The relative level of pro- and anti-apoptotic proteins plays an important role in regulating the cell death and survival.

Experimental evidence obtained in this study will provide useful information in understanding the functional mechanism and physiological significance of MDC or ADAM proteins composed of functionally distinct multidomains.

The cDNA sequence of halysase has been deposited in the GenBank database under the accession number AY149647. This work was supported by the Brain Korea 21 Project in 2003.

REFERENCES

1. Boudreau, N.J. and Jones, P.L. (1999) Extracellular matrix and integrin signaling: the shape of things to come. *Biochem. J.* **339**, 481–488
2. Werb, Z. (1997) ECM and cell surface proteolysis: regulating cellular ecology. *Cell* **91**, 439–442
3. Varner, J.A. and Cheresh, D.A. (1996) Integrins and cancer. *Curr. Opin. Cell Biol.* **8**, 724–730
4. Liu, W., Ahmad, S.A., Reinmuth, N., Shaheen, R.M., Jung, Y.D., Fan, F., and Ellis, L.M. (2000) Endothelial cell survival and apoptosis in the tumor vasculature. *Apoptosis* **5**, 323–328
5. Brooks, P.C., Montgomery, A.M., Rosenfeld, M., Reisfeld, R.A., Hu, T., Klier, G., and Cheresh, D.A. (1994) Integrin αvβ3 antagonists promote tumor regression by inducing apoptosis of angiogenic blood vessels. *Cell* **79**, 1157–1164
6. Stromblad, S. and Cheresh, D.A. (1996) Integrins, angiogenesis and vascular cell survival. *Chem. Biol.* **3**, 881–885
7. Hite, L.A., Jia, L.G., Bjarnason, J.B., and Fox, J.W. (1994) cDNA sequences for four snake venom metalloproteinases: structure, classification, and their relationship to mammalian reproductive proteins. *Arch. Biochem. Biophys.* **308**, 182–191
8. Matsui, T., Fujimura, Y., and Titani, K. (2000) Snake venom proteases affecting hemostasis and thrombosis. *Biochim. Biophys. Acta.* **1477**, 146–156
9. Yamada, D., Shin, Y., and Morita, T. (1999) Nucleotide sequence of a cDNA encoding a common precursor of disintegrin flavostatin and hemorrhagic factor HR2a from the venom of *Trimeresurus flavoviridis*. *FEBS Lett.* **451**, 299–302
10. Masuda, S., Hayashi, H., and Araki, S. (1998) Two vascular apoptosis-inducing proteins from snake venom are members of the metalloprotease/disintegrin family. *Eur. J. Biochem.* **253**, 36–41
11. Masuda, S., Hayashi, H., Atoda, H., Morita, T., and Araki, S. (2001) Purification, cDNA cloning and characterization of the vascular apoptosis-inducing protein, HV1, from *Trimeresurus flavoviridis*. *Eur. J. Biochem.* **268**, 3339–3345
12. Masuda, S., Ohta, T., Kaji, K., Fox, J.W., Hayashi, H., and Araki, S. (2000) cDNA cloning and characterization of vascular apoptosis-inducing protein 1. *Biochem. Biophys. Res. Commun.* **278**, 197–204
13. Wu, W.B., Chang, S.C., Liau, M.Y., and Huang, T.F. (2001) Purification, molecular cloning and mechanism of action of graminelysin I, a snake-venom-derived metalloproteinase that induces apoptosis of human endothelial cells. *Biochem. J.* **357**, 719–728
14. Wang, S.H., Shen, X.C., Yang, G.Z., and Wu, X.F. (2003) cDNA cloning and characterization of Agkistin, a new metalloproteinase from *Agkistrodon halys*. *Biochem. Biophys. Res. Commun.* **301**, 298–303
15. Blobel, C.P., Wolfsberg, T.G., Turck, C.W., Myles, D.G., Primakoff, P., and White, J.M. (1992) A potential fusion peptide and an integrin ligand domain in a protein active in sperm-egg fusion. *Nature* **356**, 248–252
16. Peschon, J.J., Slack, J.L., Reddy, P., Stocking, K.L., Sunnarborg, S.W., Lee, D.C., Russell, W.E., Castner, B.J., Johnson, R.S., Fitzner, J.N., Boyce, R.W., Nelson, N., Kozlosky, C.J., Wolfson, M.F., Rauch, C.T., Cerretti, D.P., Paxton, R.J., March, C.J., and Black, R.A. (1998) An essential role for ectodomain shedding in mammalian development. *Science* **282**, 1281–1284
17. Yagami-Hiromasa, T., Sato, T., Kurisaki, T., Kamijo, K., Nabeshima, Y., and Fujisawa-Sehara, A. (1995) A metalloprotease-disintegrin participating in myoblast fusion. *Nature* **377**, 652–656
18. Pan, D. and Rubin, G.M. (1997) Kuzbanian controls proteolytic processing of Notch and mediates lateral inhibition during Drosophila and vertebrate neurogenesis. *Cell* **90**, 271–280
19. Fairbanks, G., Steck, T.L., and Wallach, D.F. (1971) Electrophoretic analysis of the major polypeptides of the human erythrocyte membrane. *Biochemistry* **10**, 2606–2617
20. Jeon, O.H. and Kim, D.S. (1999) Molecular cloning and functional characterization of a snake venom metalloprotease. *Eur. J. Biochem.* **263**, 526–533
21. You, W.K., Jang, Y.J. Chung, K.H., and Kim, D.S. (2003) A novel disintegrin-like domain of a high molecular weight metalloprotease inhibits platelet aggregation. *Biochem. Biophys. Res. Commun.* **309**, 637–642
22. Jeon, O.H. and Kim, D.S. (1999) Cloning, expression, and characterization of a cDNA encoding snake venom metalloprotease. *Biochem. Mol. Biol. Int.* **47**, 417–425
23. Jaffe, E.A., Nachman, R.L., Becker, C.G., and Minick, C.R. (1973) Culture of human endothelial cells derived from umbilical veins. Identification by morphologic and immunologic criteria. *J. Clin. Invest.* **52**, 2745–2756
24. Sahni, A. and Francis, C.W. (2000) Vascular endothelial growth factor binds to fibrinogen and fibrin and stimulates endothelial cell proliferation. *Blood* **96**, 3772–3778
25. Kang, I.C., Lee, Y.D., and Kim, D.S. (1999) A novel disintegrin salmosin inhibits tumor angiogenesis. *Cancer Res.* **59**, 3754–3760
26. Yamagishi, S., Yonekura, H., Yamamoto, Y., Katsuno, K., Sato, F., Mita, I., Ooka, H., Satozawa, N., Kawakami, T., Nomura, M., and Yamamoto, H. (1997) Advanced glycation end products-driven angiogenesis *in vitro*. Induction of the growth and tube formation of human microvascular endothelial cells through autocrine vascular endothelial growth factor. *J. Biol. Chem.* **272**, 8723–8730

Downloaded from http://jb.oxfordjournals.org/ at Changhua Christian Hospital on September 29, 2012

27. Hite, L.A., Shannon, J.D., Bjarnason, J.B., and Fox, J.W. (1992) Sequence of a cDNA clone encoding the zinc metalloproteinase hemorrhagic toxin e from *Crotalus atrox*: evidence for signal, zymogen, and disintegrin-like structures. *Biochemistry* **31**, 6203–6211
28. Selistre de Araujo, H.S., and Ownby, C.L. (1995) Molecular cloning and sequence analysis of cDNAs for metalloproteinases from broad-banded copperhead *Agkistrodon contortrix laticinctus*. *Arch. Biochem. Biophys.* **320**, 141–148
29. Bikfalvi, A., Klein, S., Pintucci, G., and Rifkin, D.B. (1997) Biological roles of fibroblast growth factor-2. *Endocr. Rev.* **18**, 26–45
30. Gross, A., McDonnell, J.M., and Korsmeyer, S.J. (1999) BCL-2 family members and the mitochondria in apoptosis. *Genes Dev.* **13**, 1899–1911
31. Saelman, E.U., Keely, P.J., and Santoro, S.A. (1995) Loss of MDCK cell $\alpha 2\beta 1$ integrin expression results in reduced cyst formation, failure of hepatocyte growth factor/scatter factor-induced branching morphogenesis, and increased apoptosis. *J. Cell Sci.* **108**, 3531–3540
32. Zhang, Z., Vuori, K., Reed, J.C., and Ruoslahti, E. (1995) The alpha 5 beta 1 integrin supports survival of cells on fibronectin and up-regulates Bcl-2 expression. *Proc. Natl Acad. Sci. USA* **92**, 6161–6165
33. Blobel, C.P. and White, J.M. (1992) Structure, function and evolutionary relationship of proteins containing a disintegrin domain. *Curr. Opin. Cell. Biol.* **4**, 760–765
34. McLane, M., A., Marcinkiewicz, C., Vijay-Kumar, S., Wierzbicka-Patynowski, I., and Niewiarowski, S. (1998) Viper venom disintegrins and related molecules. *Proc. Soc. Exp. Biol. Med.* **219**, 109–119
35. Juliano, D., Wang, Y., Marcinkiewicz, C., Rosenthal, L.A., Stewart, G.J., and Niewiarowski, S. (1996) Disintegrin interaction with $\alpha V\beta 3$ integrin on human umbilical vein endothelial cells: expression of ligand-induced binding site on $\beta 3$ subunit. *Exp. Cell Res.* **225**, 132–142
36. Hong, S.Y., Koh, Y.S., Chung, K.H., and Kim, D.S. (2002) Snake venom disintegrin, saxatilin, inhibits platelet aggregation, human umbilical vein endothelial cell proliferation, and smooth muscle cell migration. *Thromb. Res.* **105**, 79–86
37. Kamiguti, A.S., Hay, C.R., and Zuzel, M. (1996) Inhibition of collagen-induced platelet aggregation as the result of cleavage of $a\alpha 2\beta 1$-integrin by the snake venom metalloproteinase jararhagin. *Biochem. J.* **320**, 635–641
38. Zigrino, P., Kamiguti, A.S., Eble, J., Drescher, C., Nischt, R., Fox, J.W., and Mauch, C. (2002) The reprolysin jararhagin, a snake venom metalloproteinase, functions as a fibrillar collagen agonist involved in fibroblast cell adhesion and signaling. *J. Biol. Chem.* **277**, 40528–40535
39. Laurie, G.W., Bing, J.T., Kleinman, H.K., Hassell, J.R., Aumailley, M., Martin, G.R., and Feldmann, R.J. (1986) Localization of binding sites for laminin, heparan sulfate proteoglycan and fibronectin on basement membrane (type IV) collagen. *J. Mol. Biol.* **189**, 205–216
40. Frisch, S.M. and Ruoslahti, E. (1997) Integrins and anoikis. *Curr. Opin. Cell Biol.* **9**, 701–706
41. Frisch, S.M. and Screaton, R.A. (2001) Anoikis mechanisms. *Curr. Opin. Cell Biol.* **13**, 555–562
42. Araki, S., Masuda, S., Maeda, H., Ying, M.J., and Hayashi, H. (2002) Involvement of specific integrins in apoptosis induced by vascular apoptosis-inducing protein 1. *Toxicon* **40**, 535–542

Downloaded from http://jb.oxfordjournals.org/ at Changhua Christian Hospital on September 29, 2012